International Journal of Heat and Mass Transfer 52 (2009) 2102–2109

Contents lists available at ScienceDirect

International Journal of Heat and Mass Transfer

journal homepage: www.elsevier.com/locate/ijhmt

Analysis of the 3-omega method for thermal conductivity measurement

Hainan Wang, Mihir Sen *

Department of Aerospace and Mechanical Engineering, University of Notre Dame, Notre Dame, IN 46556, USA

ARTICLE INFO

Article history:
Received 29 July 2008
Received in revised form 29 October 2008
Available online 26 December 2008

Keywords:
Thermal conductivity
3-omega method

ABSTRACT

The 3ω method for measurement of thermal conductivity of a solid usually consists of a strip heater above a substrate, and the method is based on an approximate solution of the heat conduction problem in which the heater thickness is neglected. We establish a two-dimensional heat conduction model for the heater-on-substrate 3ω method which takes into account the finite thickness of the heater. Analytical solutions for the finite-heater problem and the vanishing heater-thickness problem are presented utilizing the method of separation of variables. It is found that neglecting the heater thickness is not accurate at low or high frequencies, but works well in between. This frequency range becomes narrower when the heater thickness increases.

1. Introduction

The 3ω method originated from Corbino [1,2] who discovered the small third-harmonic voltage component while applying an alternating current through a heater. Later, it was used to measure the specific heat of the heater itself [3,4]. The method became popular after it was developed to measure the specific heat of substrate materials [5–7], where a one-dimensional heater-on-substrate conduction model with an applied heat flux was set up which was strictly valid for an ideal, infinite, and planar heater. A similar model was used for the simultaneous measurement of both thermal conductivity and specific heat [8]. A seminal contribution was made by Cahill et al. [9,10] on obtaining an analytical solution for a vanishingly thin but finite-width heater. The analytical solution for a line heater on a substrate [11] was integrated to give the solution for the heater of finite width in integral form [10]. An approximation for the integral solution, which is commonly used, was also obtained for small frequencies [10].

A few authors have extended this approach. The integral solution for finite-width heater was investigated and a formula was derived for heat capacity measurement at the same frequency range as the conductivity measurement [12]. Moon et al. [13] showed that a much simpler formula exists at the high-frequency limit which can be used for specific heat measurement. The integral solutions have also been extended to measure the thermal properties of thin films [14–21] and liquid materials [13,22–24]. Other than heater-on-substrate configurations, several authors have also developed the 3ω method for suspended wires, such as nanowires [25] and nanotubes [26–29]. A general analysis on the thermal and voltage response for both suspended wire and narrow planar heater, and the difference between the current- and voltage-driven setups, was also discussed [30].

Few studies have solved the heater-on-substrate problem, which is the basis of the 3ω method, by starting from anything other than the original line heater solution [9,10]. The two-dimensional conduction problem for 3ω method with an imposed heat flux was solved using a Green's function [31]. The three-dimensional conduction problem was also solved using the integral transform method and the heat flux boundary condition [32]. It was pointed out that the linear formula is not valid at very low frequencies and another approximate formula, based on an analytical solution, for thermal conductivity calculation at very low frequencies was given [32].

All these studies have neglected the thickness of the heater (normal to the substrate). Birge and Nagel [6] claimed that the heater thickness can be neglected if it is small compared to the penetration depth and if the heat stored in the heater itself can be ignored. However, no analysis was given there. Jonsson and Andersson [33] utilized the finite element technique to simulate the one-dimensional 3ω method [5–7]. They considered the heater thickness in their model and their results showed that there is a low-frequency limit for the validity of the model and that, at high frequencies, the finite thickness of the heater also causes a deviation from the theoretical prediction. It should be pointed out that they assumed a constant temperature at the interface between the substrate and the heater. Jacquot et al. [34] numerically simulated the problem by a finite-volume technique, in which they took into account the heater length and thickness, and the isothermal and adiabatic boundary conditions of the substrate. They also noticed that there is a decrease of the temperature oscillation from the integral solution at small frequencies. Borca-Tasciuc et al. [35] incorporated the heater thickness and heat capacity in their analytical model, while neglecting the heat conduction within

* Corresponding author. Tel.: +1 574 631 5975; fax: +1 657 631 8341.
E-mail address: mihir.sen.1@nd.edu (M. Sen).

0017-9310/$ - see front matter © 2008 Elsevier Ltd. All rights reserved.
doi:10.1016/j.ijheatmasstransfer.2008.10.020

Nomenclature

a and b	heater thickness and width defined in Fig. 1(a) (m)
c and d	dimensions of substrate defined in Fig. 1(a) (m)
A, C, and D	non-dimensional distances
$H(\cdot)$	Heaviside function
I_0	alternating current amplitude (A)
k	thermal conductivity (W/m K)
K	thermal conductivity ratio between substrate and heater
L	coefficient vector
M	coefficient matrix
P	power generated per unit length (W/m)
q''	heat flux (W/m^2)
R	coefficient vector
t	non-dimensional time
t^*	dimensional time (s)
T	non-dimensional temperature
T^*	dimensional temperature (K)
T_0^*	reference temperature (K)
(x,y)	non-dimensional Cartesian coordinates
(x^*,y^*)	dimensional Cartesian coordinates (m,m)

Greek symbols

α	thermal diffusivity (m^2/s)
β	thermal diffusivity ratio between substrate and heater
$\theta_{h,s}^{c,s}$	amplitude of non-dimensional temperature oscillation
χ	ratio between heater width b and the penetration depth $\sqrt{\alpha_s/2\omega^*}$
ω^*	frequency (rad/s)

Subscripts

h	heater
s	substrate

Superscripts

c	in-phase component
s	out-of-phase component

Other symbols

$\bar{\cdot}$	time average
$\langle\cdot\rangle$	spatial average

the heater. They concluded that for a larger heat capacity of the heater, the maximum working frequency of 3ω method will decrease. It was claimed that the main drawback of the 3ω method is the requirement for the heater to be long and thin and the uncertainties associated with that, but no analysis was provided [36].

Although the 3ω method is extensively used for thermal conductivity measurement, the formulas generally used are based on the zero heater-thickness approximation. It is therefore necessary to provide a complete analysis of the problem to determine the limits of its applicability. In this paper, we study a two-dimensional conduction model for the heater-on-substrate 3ω method, in which the heater thickness is non-zero. The analytical solution is obtained using the method of separation of variables. The aim is to provide a solid theoretical foundation for 3ω method.

2. Formulation of problem

The experimental device consists of a metal heater on a semi-infinite substrate that is schematically shown in cross-section in Fig. 1(a). The thermal conductivity of the substrate is to be measured. An alternating current, $I_0\cos\omega^* t^*$, is made to flow through the heater into the plane of the paper, where I_0 is the magnitude, ω^* is the frequency of the current, and t^* is time. Therefore, the instantaneous Joule heat generated in the heater per unit time per unit length is $P\cos^2\omega^* t^* = P(1+\cos 2\omega^* t^*)/2$, where $P = I_0^2 R$ is the power per unit length, and R is the heater resistance per unit length. The voltage drop across the heater is measured and from that, by resistance thermometry, the spatial average of the oscillatory temperature of the heater is deduced. The relation between the amplitude of the heater spatially-averaged temperature oscillation and the frequency of the alternating current depends on the thermal conductivity and diffusivity of the substrate material, and so their values can be deduced.

2.1. Finite heater thickness

2.1.1. Geometry

The heater in Fig. 1(a) is the rectangle $DEE'D'$, and the substrate whose thermal conductivity is to be measured is $BCC'B'$. Due to symmetry along the line AGF, we only need to consider the half to the right of it. For typical values used in the experiments, the length of the specimen into the paper is also large enough compared with the thickness FG and width DD' of the heater, so the problem can be considered to be two-dimensional. We take $FG = a$, $EF = b$, $CG = c$, and $GA = d$, where c and d are two orders of magnitude larger than b, so the boundaries AB and BC are far enough away from the heater so as to be assumed isothermal. Thus

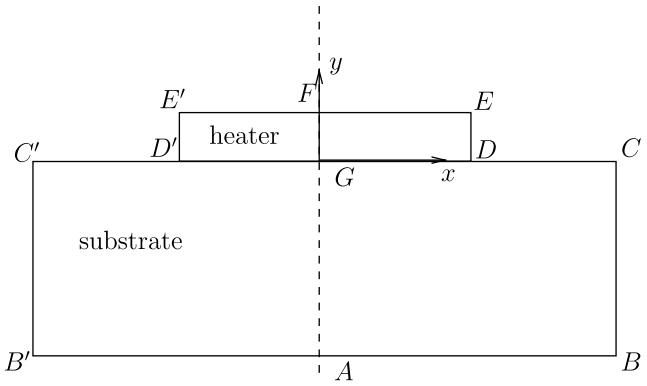

(a) Heater of finite thickness.

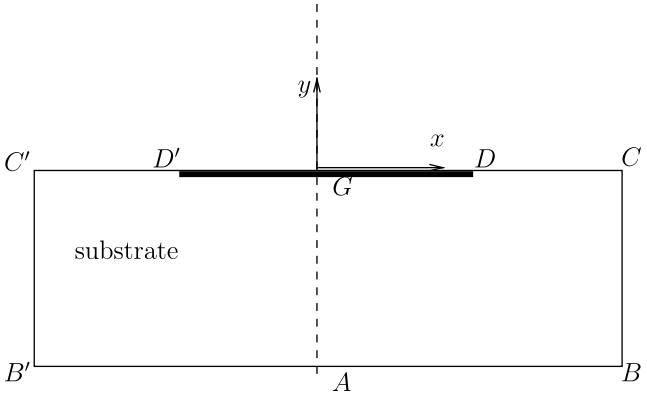

(b) Heater of zero thickness.

Fig. 1. Heater on substrate (not to scale).

the boundary conditions on the temperature $T^*(x,y,t)$ are taken to be the following: isothermal ($T^* = T_0^*$) on *AB* and on *BC*; adiabatic (normal derivative zero) on *CD*, *DE*, *EF*, *FG* and *GA*. At the interface between the heater and the substrate, *GD*, the temperature and the heat flux on either side should match.

2.1.2. Governing equations

The first task is to determine the temperature distribution in the heater and substrate using the unsteady conduction equation. Since the temperature oscillation is small, the thermal conductivities of both materials can be assumed to be constant. The volumetric heat generation within the heater is $P(1+\cos 2\omega^* t^*)/4ab$ per unit length. The governing equations for conduction in the heater and substrate are

$$\frac{\partial^2 T_h^*}{\partial x^{*2}} + \frac{\partial^2 T_h^*}{\partial y^{*2}} + \frac{P}{4abk_h}(1+\cos 2\omega^* t^*) = \frac{1}{\alpha_h}\frac{\partial T_h^*}{\partial t^*}, \tag{1a}$$

$$\frac{\partial^2 T_s^*}{\partial x^{*2}} + \frac{\partial^2 T_s^*}{\partial y^{*2}} = \frac{1}{\alpha_s}\frac{\partial T_s^*}{\partial t^*}, \tag{1b}$$

where (x^*,y^*) are the Cartesian coordinates shown in Fig. 1(a), $T_h^*(x^*,y^*,t^*)$ and $T_s^*(x^*,y^*,t^*)$ are the temperatures in the heater and substrate, respectively, α_h and k_h are the thermal diffusivity and conductivity, respectively, of the heater material, and α_s and k_s are those of the substrate material.

Using the non-dimensional variables $T_{h,s} = (T_{h,s}^* - T_0^*)(4ak_h/bP)$, $x = x^*/b$, $y = y^*/b$ and $t = \omega^* t^*$, we get

$$\frac{\partial^2 T_h}{\partial x^2} + \frac{\partial^2 T_h}{\partial y^2} + (1+\cos 2t) = \chi^2\beta\frac{\partial T_h}{\partial t}, \tag{2a}$$

$$\frac{\partial^2 T_s}{\partial x^2} + \frac{\partial^2 T_s}{\partial y^2} = \chi^2\frac{\partial T_s}{\partial t}, \tag{2b}$$

where $\chi = \sqrt{2\omega^* b^2/\alpha_s}$ and $\beta = \alpha_s/\alpha_h$. The lengths in Fig. 1(a) are non-dimensionalized as $A = a/b$, $C = c/b$ and $D = d/b$.

We can separate the time-independent and oscillatory parts of the temperature as

$$T_h = \overline{T}_h(x,y) + \theta_h^c(x,y)\cos 2t + \theta_h^s(x,y)\sin 2t, \tag{3a}$$

$$T_s = \overline{T}_s(x,y) + \theta_s^c(x,y)\cos 2t + \theta_s^s(x,y)\sin 2t, \tag{3b}$$

where $\overline{T}_{h,s}$ represents the *time average* of the non-dimensional temperature, and $\theta_{h,s}^c$ are the amplitude of the non-dimensional temperature oscillation around the time average that is in phase with the current, and $\theta_{h,s}^s$ is that which is 90° out of phase.

Substituting Eqs. (3a,b) in Eqs. (2a,b) and averaging over one period, we get

$$\frac{\partial^2 \overline{T}_h}{\partial x^2} + \frac{\partial^2 \overline{T}_h}{\partial y^2} + 1 = 0, \tag{4a}$$

$$\frac{\partial^2 \overline{T}_s}{\partial x^2} + \frac{\partial^2 \overline{T}_s}{\partial y^2} = 0. \tag{4b}$$

Substituting Eqs. (3a,b) again in Eqs. (2a,b), subtracting Eqs. (4a,b), and collecting the cosine and sine terms, we get

$$\frac{\partial^2 \theta_h^c}{\partial x^2} + \frac{\partial^2 \theta_h^c}{\partial y^2} + 1 = \chi^2\beta\theta_h^s, \tag{5a}$$

$$\frac{\partial^2 \theta_h^s}{\partial x^2} + \frac{\partial^2 \theta_h^s}{\partial y^2} = -\chi^2\beta\theta_h^c, \tag{5b}$$

for the heater and

$$\frac{\partial^2 \theta_s^c}{\partial x^2} + \frac{\partial^2 \theta_s^c}{\partial y^2} = \chi^2\theta_s^s, \tag{5c}$$

$$\frac{\partial^2 \theta_s^s}{\partial y^2} + \frac{\partial^2 \theta_s^s}{\partial y^2} = -\chi^2\theta_s^c, \tag{5d}$$

for the substrate, respectively. In the 3ω method, only the oscillatory amplitudes θ_h^c, θ_h^s, θ_s^c and θ_s^s are of interest.

The *spatial average* of the heater temperature oscillation can be defined as

$$\langle\theta_h^{c,s}\rangle = \frac{1}{A}\int_0^A\int_0^1 \theta_h^{c,s}(x,y)\,dx\,dy. \tag{6}$$

2.1.3. Boundary conditions

At the adiabatic boundaries of the heater, the normal derivative of $\theta_h^{c,s}$ should vanish. For the substrate, at the isothermal boundaries, $\theta_s^{c,s} = 0$, and at the adiabatic boundaries the normal derivative of $\theta_h^{c,s}$ is zero. At the interface between the heater and the substrate $\theta_h^{c,s} = \theta_s^{c,s}$ and $\partial\theta_h^{c,s}/\partial y = K\partial\theta_s^{c,s}/\partial y$, where $K = k_s/k_h$.

2.2. Vanishing heater-thickness approximation

Previous authors [5–10,12–24,30–32,35,37] have simplified the problem by neglecting the heater thickness, as in Fig. 1(b); thus only the rectangular region *ABCG* has to be considered. The governing equations are then Eqs. (5c) and (5d). The only change is the boundary condition at the interface DG represented by an imposed heat flux [37]

$$q'' = \frac{P}{4b}(1+\cos 2\omega^* t^*). \tag{7}$$

Non-dimensionally this gives

$$\frac{K}{A}\frac{\partial\tilde{\theta}_s}{\partial y} = H(x) - H(x-1) \text{ at } y = 0, \tag{8}$$

where $H(\cdot)$ is the Heaviside function.

The spatial average of the temperature oscillation in this case is

$$\langle\theta_h^{c,s}\rangle = \int_0^1 \theta_s^{c,s}(x,0)\,dx. \tag{9}$$

3. Analytical solutions

3.1. Complex equations

To make the solution compact, we introduce the complex temperature oscillation variables $\tilde{\theta}_h(x,y,t) = \theta_h^c + i\theta_h^s$ and $\tilde{\theta}_s(x,y,t) = \theta_s^c + i\theta_s^s$. Eqs. (5a,b) are thus the real and imaginary parts of

$$\frac{\partial^2\tilde{\theta}_h}{\partial x^2} + \frac{\partial^2\tilde{\theta}_h}{\partial y^2} + 1 = -\mathrm{i}\beta\chi^2\tilde{\theta}_h, \tag{10a}$$

$$\frac{\partial^2\tilde{\theta}_s}{\partial x^2} + \frac{\partial^2\tilde{\theta}_s}{\partial y^2} = -\mathrm{i}\chi^2\tilde{\theta}_s. \tag{10b}$$

The boundary conditions in Section 2.1.3 now apply to the complex quantities $\tilde{\theta}_{h,s}$. For the vanishing heater-thickness problem, the governing equation is only Eq. (10b).

3.2. Finite-heater solution

Utilizing the method of separation of variables [38], the general solutions of Eq. (10a,b) subject to the boundary conditions in Section 2.1.3, but without using the interface conditions yet, can be obtained as

$$\tilde{\theta}_s(x,y) = \sum_n c_n\cos\left(p_{s,n}x\right)\left(e^{q_{s,n}y} - e^{-2q_{s,n}D}e^{-q_{s,n}y}\right), \tag{11}$$

$$\tilde{\theta}_h(x,y) = \sum_n d_n\cos(n\pi x)\left(e^{-2q_{h,n}A}e^{q_{h,n}y} + e^{-q_{h,n}y}\right) - \frac{1}{\mathrm{i}\beta\chi^2}, \tag{12}$$

where $p_{s,n} = (n+\frac{1}{2})\pi/C$, $q_{s,n}^2 = p_{s,n}^2 - \mathrm{i}\chi^2$, and $q_{h,n}^2 = n^2\pi^2 - \mathrm{i}\beta\chi^2$. For other combinations of boundary conditions, the eigenvalues and

eigenfunctions take different forms [38]. For example, for a convective boundary condition the eigenvalues have to be determined numerically from the corresponding transcendental equation.

The constants c_n and d_n will be determined from the interface conditions at $y = 0$. Equating the heat flux on both sides at the interface, we have

$$\sum_n d_n \cos(n\pi x) q_{h,n} \left(e^{-2q_{h,n}A} - 1\right)[H(x) - H(x-1)] = K \sum_n c_n \cos\left(p_{s,n}x\right) q_{s,n}\left(1 + e^{-2q_{s,n}D}\right). \tag{13}$$

Multiplying both sides by $\cos p_{s,m}x$ and integrating from $x = 0$ to C, we obtain

$$\sum_n d_n q_{h,n}\left(e^{-2q_{h,n}A} - 1\right)\gamma_{mn} = Kc_m q_{s,m}\left(1 + e^{-2q_{s,m}D}\right)C/2 \tag{14}$$

where

$$\gamma_{mn} = \frac{(-1)^n p_{s,m}\sin(p_{s,m})}{p_{s,m}^2 - n^2\pi^2}, \quad m = 0, 1, 2, \ldots \tag{15}$$

Equating the temperature at the interface, we have

$$\left(\sum_n d_n \cos(n\pi x)\left(e^{-2q_{h,n}A} + 1\right) - \frac{1}{\mathrm{i}\beta\chi^2} - \sum_n c_n \cos(p_{s,n}x)\left(1 - e^{-2q_{s,n}D}\right)\right) \times [H(x) - H(x-1)] = 0. \tag{16}$$

Multiplying both sides by $\cos(m\pi x)$ and integrating from $x = 0$ to $x = 1$, we get

$$d_0\left(e^{-2q_{h,m}A} + 1\right) - \frac{1}{\mathrm{i}\beta\chi^2} = \sum_n c_n\left(1 - e^{-2q_{s,n}D}\right)\gamma_{nm} \text{ for } m = 0, \tag{17a}$$

$$d_m\left(e^{-2q_{h,m}A} + 1\right)\frac{1}{2} = \sum_n c_n\left(1 - e^{-2q_{s,n}D}\right)\gamma_{nm} \text{ for } m \neq 0, \tag{17b}$$

where

$$\gamma_{nm} = \frac{(-1)^m p_{s,n}\sin\left(p_n\right)}{p_{s,n}^2 - m^2\pi^2}.$$

Eqs. (14) and (17a,b) form a set of complex linear equations that can be written in matrix form as

$$\mathbf{ML} = \mathbf{R}, \tag{18}$$

where, $\mathbf{M}$ is the coefficient matrix, $\mathbf{L} = \{d_0, d_1, \ldots, d_n, c_0, c_1, \ldots, c_n\}^T$, $\mathbf{R} = \{0, 0, \ldots, 0, 1/i\beta\chi^2, 0, \ldots, 0\}^T$. From this the coefficients c_n and d_n can be solved in Matlab directly using the matrix left division [39]. By substituting the heater solution Eq. (12) into Eq. (6), the expression for spatially-averaged temperature oscillation of the heater is found to be

$$\langle\tilde{\theta}_h\rangle = \frac{d_0}{A\sqrt{-\mathrm{i}\beta\chi^2}}\left(1 - e^{-2A\sqrt{-\mathrm{i}\beta\chi^2}}\right) - \frac{1}{\mathrm{i}\beta\chi^2}. \tag{19}$$

3.3. Vanishing heater-thickness approximation

By utilizing a procedure similar to that in the previous section, the solution for a heater of vanishing thickness can be obtained as

$$\tilde{\theta}_s(x, y) = \frac{2A}{KC}\sum_n \cos(p_{s,n}x)\frac{\sin\left(p_{s,n}\right)}{p_{s,n}q_{s,n}}\frac{e^{q_{s,n}y} - e^{-2q_{s,n}D}e^{-q_{s,n}y}}{1 + e^{-2q_{s,n}D}}, \tag{20}$$

where $p_{s,n}$ and $q_{s,n}$ are defined the same as in the previous section. At the interface we have

$$\tilde{\theta}_s(x, 0) = \frac{2A}{KC}\sum_n \cos(p_{s,n}x)\frac{\sin(p_{s,n})}{p_{s,n}}\frac{\tanh(q_{s,n}D)}{q_{s,n}}. \tag{21}$$

Substituting into Eq. (9), we get

$$\langle\tilde{\theta}_h\rangle = \frac{2A}{KC}\sum_n \frac{\sin^2(p_{s,n})}{p_{s,n}^2}\frac{\tanh(q_{s,n}D)}{q_{s,n}}. \tag{22}$$

3.4. Line heater integral approximation [10]

The heater-on-substrate conduction problem can also be solved by a superposition principle: starting from the solution of the temperature field for a line heater [11] at $y = 0$, $x = 0$, and then integrating it along the width of the heater to obtain the solution for a finite-width heater. The final spatially-averaged temperature oscillation of the heater is found to be

$$\langle\tilde{\theta}_h\rangle = \frac{2A}{\pi K}\int_0^\infty \frac{\sin^2(\xi b)}{\xi^2 b\sqrt{\xi^2 b^2 + \mathrm{i}\chi^2}}d\xi, \tag{23}$$

where $\langle\tilde{\theta}_h\rangle = \langle\theta_h^c\rangle + \mathrm{i}\langle\theta_h^s\rangle$. The integration is carried out numerically in Matlab using adaptive Lobatto quadrature (quadl) [39].

At low frequencies, for which $\chi \ll 1$, this can be approximated as

$$\langle\tilde{\theta}_h\rangle = \frac{2A}{\pi K}\left(-\ln\chi + \eta - \frac{\pi}{4}\mathrm{i}\right). \tag{24}$$

The value of $\eta = 0.923$ can be determined by numerical integration of Eq. (23). The thermal conductivity is then easily calculated from the slope of an experimentally-obtained $\langle\theta_h^c\rangle$ vs. $\ln\chi$ curve, i.e. from

$$\frac{d\langle\theta_h^c\rangle}{d\ln\chi} = -\frac{2A}{\pi K}. \tag{25}$$

At high frequencies, $\chi \gg 1$, Moon et al. [13] approximated Eq. (23) by

$$\langle\tilde{\theta}_h\rangle = \frac{A}{K\chi}e^{-\mathrm{i}\pi/4}. \tag{26}$$

4. Results

The following numerical values have been used to illustrate the computations. The heater is taken to be aluminum for which the bulk properties are $k_h = 236$ W/m K, and $\alpha_h = 9.63 \times 10^{-5}$ m^2/s. The substrate is SiO_2 for which $k_s = 1.35$ W/m K, and $\alpha_s = 8.4 \times 10^{-7}$ m^2/s. The geometric parameters are $b = 20$ μm and $c = d = 3$ mm, while the thickness of the heater will be taken to be in the range $50 \leqslant a \leqslant 3000$ nm. Since the solution is in the form of an infinite series, the total number of terms must be chosen to maintain a certain accuracy. For a smaller ratio of a/b or for higher frequencies, the number of terms must be larger. In all cases here, the number of terms is taken to be 1500 and 1000 for the finite- and vanishing heater-thickness solutions, respectively. It is found that further increase in the number of terms to 2000 only results in a change of less than 1% and 0.5%, respectively.

The in-phase and out-of-phase spatially-averaged temperature oscillations of the heater $\langle\theta_h^{c,s}\rangle$ can be plotted as a function of χ, and the slope $d\langle\theta_h^c\rangle/d\ln\chi$ can be obtained respectively from Eqs. (19), (22), (23), (24) or (25). It is noticed that there is an oscillatory behavior for the finite-heater solution at very small frequencies ($\chi \lesssim 2 \times 10^{-3}$), which can be seen more clearly from the slope figure. This phenomenon becomes more significant when A is small ($A \lesssim 0.005$).

4.1. Low-frequency region

All the low-frequency data are plotted in semi-log scale in accordance with Eq. (24). Comparison between Eq. (24) and the integral

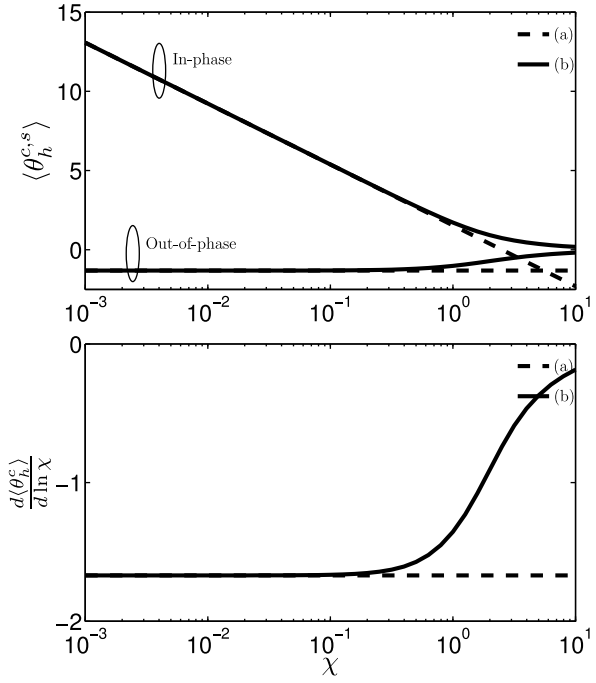

Fig. 2. Comparison between line heater linear solution Eq. (24) and line heater integral solution Eq. (23) in temperature and its slope. (a) Eq. (24) and (b) Eq. (23).

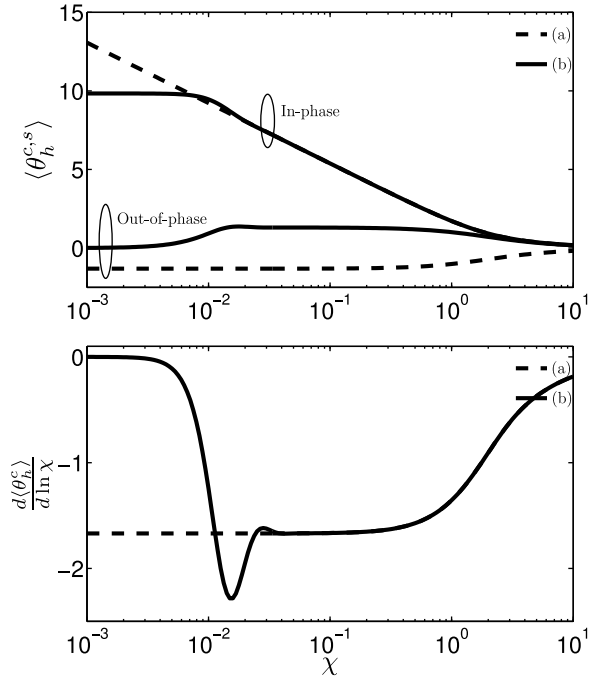

Fig. 3. Comparison between line heater integral solution Eq. (23) and vanishing heater-thickness solution Eq. (22) in temperature and its slope. (a) Eq. (23) and (b) Eq. (22).

solution Eq. (23) is shown in Fig. 2. At low frequencies ($\chi \lesssim 0.2$), both the amplitude and the slope agree quite well. The comparison between the integral solution Eq. (23) and the vanishing-thickness solution Eq. (22), is shown in Fig. 3. The in-phase components from the these two have almost the same amplitude when $\chi \gtrsim 0.02$. At smaller frequencies, the line heater integral approach breaks down since Eq. (23) becomes unbounded as $\chi \to 0$, while the correct result should be finite as is given by the vanishing-thickness solution. Jacquot et al. [34] attributed this discrepancy to the transverse heat flow and heat capacitance of the heater, but the vanishing-thickness solution presented here also makes the same assumptions and yields a reasonable value. When $\chi \gtrsim 0.02$, the amplitudes of the out-of-phase component from the integral solution and vanishing-thickness solution also agree. However, the integral solution Eq. (23) gives a negative value (Cahill [10] and Lee and Kwun [12] plotted it as positive although their formula gives a negative one), which basically means a different definition of the phase angle. When $\chi \lesssim 0.02$, the out-of-phase component predicted by the integral solution is also wrong because at $\chi = 0$, the current becomes DC, and thus the out-of-phase component should be zero, as is verified by the vanishing-thickness solution. From Fig. 3, it is seen that the slopes of the integral solution and vanishing-thickness solution agree when $\chi \gtrsim 3.5 \times 10^{-2}$. The linear relation Eq. (24) is accurate only when $3.5 \times 10^{-2} \lesssim \chi \lesssim 0.2$.

The purpose of the present paper is to investigate the effect of the finite thickness of the heater. A typical heater thickness used in experiments is around $a = 300$ nm for which $A = 0.015$. For this thickness, Fig. 4 shows that at low frequencies, the vanishing heater-thickness solution, Eq. (22), agrees well with the finite-heater solution, Eq. (19), except that the in-phase component is slightly smaller. The slopes agree when $\chi \gtrsim 0.02$. Again, the linear relation is valid when $3.5 \times 10^{-2} \lesssim \chi \lesssim 0.2$. Fig. 5 shows the result for a smaller thickness of $a = 50$ nm, which corresponds to $A = 2.5 \times 10^{-3}$; it is seldom below this in experiments. The vanishing heater-thickness solution now agrees better with the finite-heater solution in both amplitude and slope, but the linear region still does not change much. We further increase the thickness of the heater to $a = 3000$ nm, which corresponds to $A = 0.15$. The results are shown in Fig. 6. It is seen that the approximate solution deviates more from the finite-heater solution. The approximate solution predicts that there is always a linear relation at a certain frequency range, however, the finite-heater solution proves that the linear relation is accurate only within a narrower frequency region when the heater thickness increases ($3.5 \times 10^{-2} \lesssim \chi \lesssim 0.1$ for this case). For all cases considered above, the out-of-phase components from these two solutions agree well at this low-frequency range.

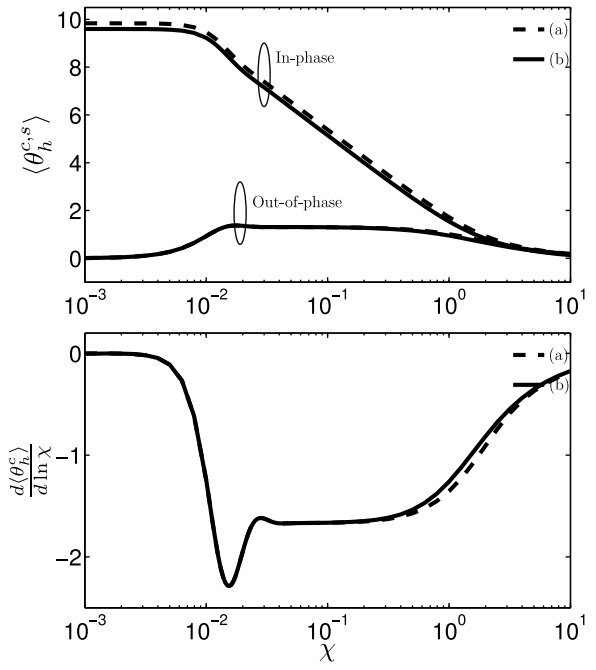

Fig. 4. Comparison between vanishing heater-thickness solution Eq. (22) and finite-heater solution Eq. (19) in temperature and its slope, with $A = 0.015$. (a) Eq. (22) and (b) Eq. (19).

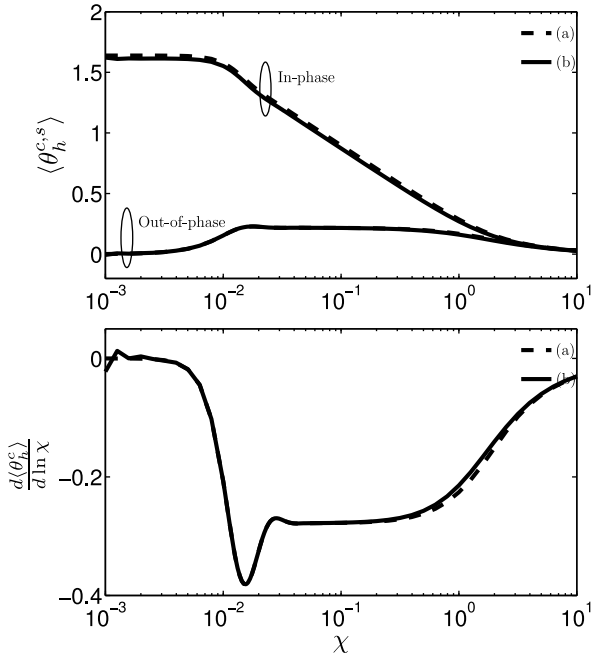

Fig. 5. Comparison between vanishing heater-thickness solution Eq. (22) and finite-heater solution Eq. (19) in temperature and its slope, with $A = 0.0025$. (a) Eq. (22) and (b) Eq. (19).

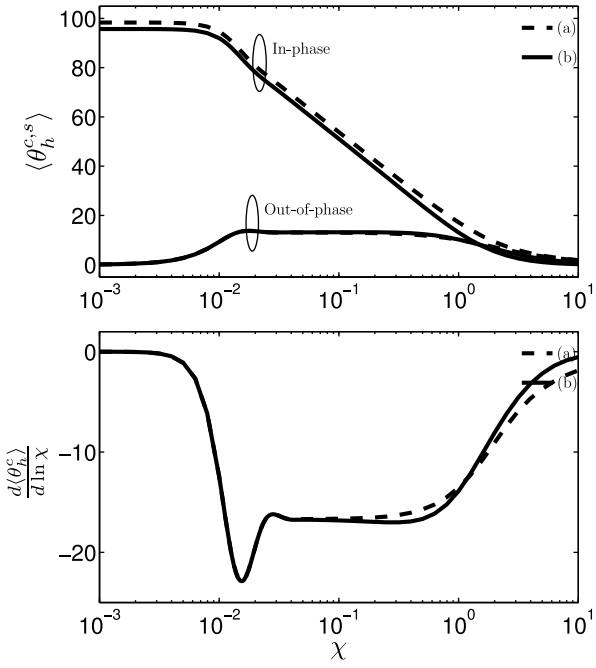

Fig. 6. Comparison between vanishing heater-thickness solution Eq. (22) and finite-heater solution Eq. (19) in temperature and its slope, with $A = 0.15$. (a) Eq. (22) and (b) Eq. (19).

4.2. High-frequency region

Eq. (26) suggests that the high-frequency data should be plotted in log–log scale. In Fig. 7, it is seen that the approximation Eq. (26) agrees with integral solution, Eq. (23), only at very high frequencies. The integral solution gives the same amplitude as the vanishing-thickness solution, Eq. (22), but again with a different sign for the out-of-phase component.

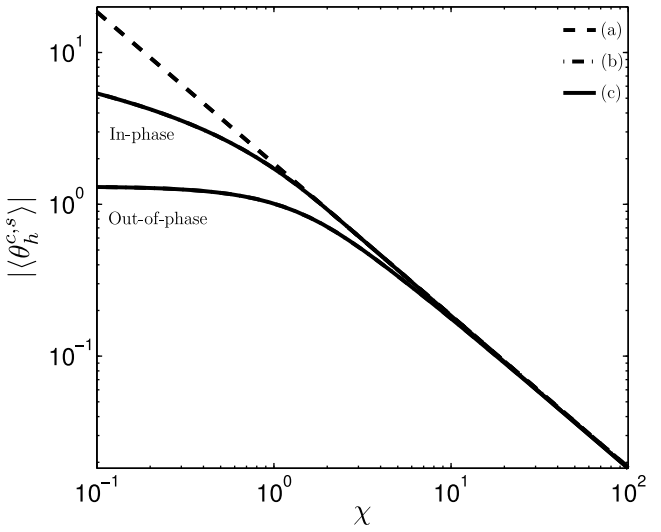

Fig. 7. Comparison among Moon's formula Eq. (26), line heater integral solution Eq. (23) and vanishing heater-thickness solution Eq. (22) in temperature amplitude at high frequencies, with $A = 0.015$. (a) Eq. (26), (b) Eq. (23) and (c) Eq. (22).

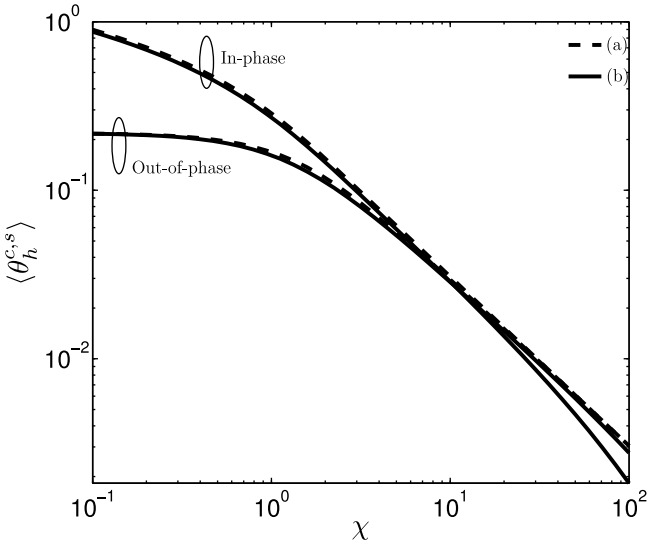

Fig. 8. Comparison between vanishing heater-thickness solution Eq. (22) and finite-heater solution Eq. (19) in temperature amplitude at high frequencies, with $A = 0.0025$. (a) Eq. (22) and (b) Eq. (19).

The comparison between vanishing-thickness solution, Eq. (22), and the finite-heater solution, Eq. (19), is shown in Figs. 8–10. It is seen that a significant difference exists between these two solutions. For the approximate solution the in-phase and out-of-phase components become the same at high frequencies, and are inversely proportional to χ. However, the finite-heater solution does not behave in that fashion, and the difference between the two solutions increases with heater thickness. Even at the very small thickness of $A = 0.0025$, as shown in Fig. 8, there is still a significant discrepancy for the in-phase component. This needs to be taken into account when using direct extensions of the integral solution, Eq. (23), for measurements at high frequencies [13,18].

5. Conclusions

A two-dimensional heat conduction model for the heater-on-substrate 3ω thermal-conductivity-measurement method is

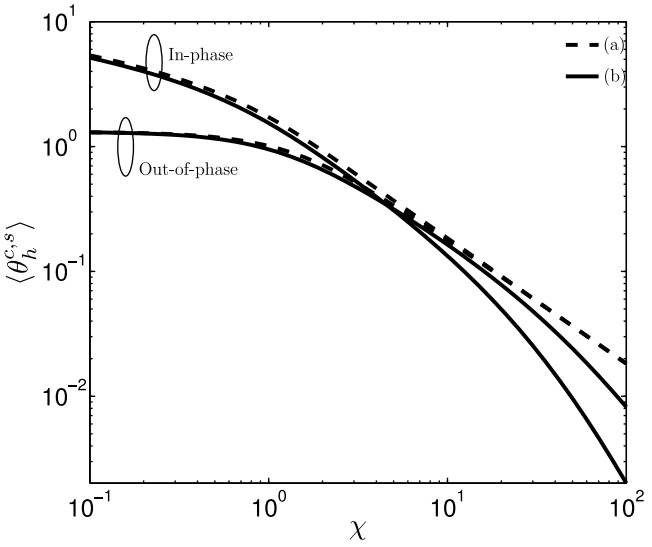

Fig. 9. Comparison between vanishing heater thickness solution Eq. (22) and finite-heater solution Eq. (19) in temperature amplitude at high frequencies, with $A = 0.015$. (a) Eq. (22) and (b) Eq. (19).

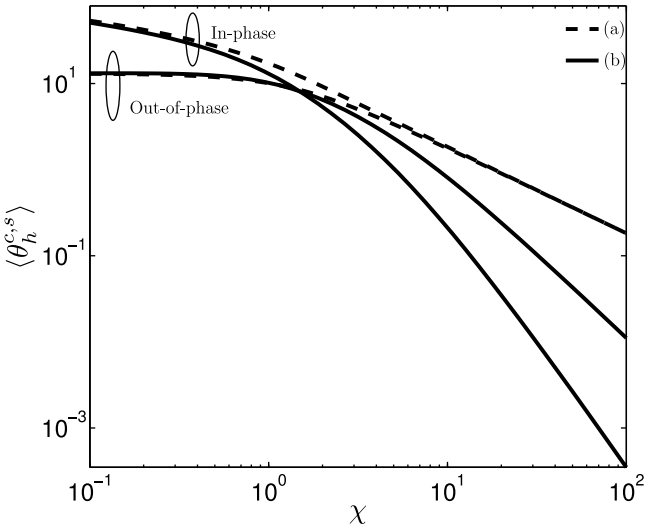

Fig. 10. Comparison between vanishing heater-thickness solution Eq. (22) and finite-heater solution Eq. (19) in temperature amplitude at high frequencies, with $A = 0.15$. (a) Eq. (22) and (b) Eq. (19).

solved for a finite thickness of the heater. A vanishing heater-thickness solution for this problem is also obtained. The solutions obtained by separation of variables are in the form of infinite series, and their coefficients are the solution of a linear matrix equation which is determined by the interface boundary condition.

The previous solution based on line-heater integral [10] agrees almost perfectly with the vanishing heater-thickness solution, except at very low frequencies. While the heater thickness is neglected in both of these two solutions, they predict a wrong behavior at high frequencies. The effect of heater thickness is of great interest and is investigated here. At low frequencies, the out-of-phase component of the vanishing heater-thickness solution agrees well with the finite-heater solution. The in-phase component has a smaller magnitude than that predicted by the finite-heater solution, but the slopes of the curves are the same. The linear relation Eq. (24) is accurate within a certain region, and this region becomes narrower as the thickness increases. However, at high frequencies there is always a disagreement between the vanishing heater-thickness approximation and finite-heater solution, and the relative difference also increases with the heater thickness. The overall conclusion is that the line-heater integral solutions, Eqs. (23) and (24), are indeed valid as long as the frequency is between a lower and an upper limit if the heater thickness is small; otherwise, the heater thickness should be considered. The analytical solution obtained here provides a theoretical basis for the evaluation of the design of a 3ω measurement setup.

Acknowledgement

The authors thank Dr. Wenjun (Katherine) Liu for introducing them this measurement technique.

References

[1] O.M. Corbino, Thermal oscillations in lamps of thin fibers with alternating current flowing through them and the resulting effect on the rectifier as a result of the presence of even-numbered harmonics, Phys. Z. 11 (1910) 413–417.
[2] O.M. Corbino, Periodic resistance changes of fine metal threads which are brought together by alternating streams as well as deduction of their thermo characteristics at high temperatures, Phys. Z. 12 (1911) 292–295.
[3] L.A. Rosenthal, Thermal response of bridewire used in electroexplosive devices, Rev. Sci. Instrum. 32 (9) (1961) 1033–1036.
[4] L.R. Holland, Physical properties of Titanium III the specific heat, J. Appl. Phys. 34 (8) (1963) 2350–2357.
[5] N.O. Birge, S.R. Nagel, Specific-heat spectroscopy of the glass transition, Phys. Rev. Lett. 544 (25) (1985) 2674–2677.
[6] N.O. Birge, S.R. Nagel, Wide-frequency specific heat spectrometer, Rev. Sci. Instrum. 58 (8) (1987) 1464–1470.
[7] N.O. Birge, P.K. Dixon, N. Menon, Specific heat spectroscopy: origins status and applications of the 3ω method, Thermochim. Acta 304/305 (1997) 51–66.
[8] R. Frank, V. Drach, J. Fricke, Determination of thermal conductivity and specific heat by a combined 3ω/decay technique, Rev. Sci. Instrum. 64 (3) (1993) 760–765.
[9] D.G. Cahill, R.O. Pohl, Thermal conductivity of amorphous solids above the plateau, Phys. Rev. B 35 (8) (1987) 4067–4073.
[10] D.G. Cahill, Thermal conductivity measurement from 30 to 750 K: the 3ω method, Rev. Sci. Instrum. 61 (2) (1990) 802–808.
[11] H.S. Carslaw, J.C. Jaeger, Conduction of Heat in Solids, second ed., Oxford University Press, USA, 1986.
[12] S. Lee, S.-Il. Kwun, Heat capacity measurement of dielectric solids using a linear surface heater: application to ferroelectrics, Rev. Sci. Instrum. 65 (1994) 966–970.
[13] I.K. Moon, Y.H. Jeong, S.I. Kwun, The 3ω technique for measuring dynamic specific heat and thermal conductivity of a liquid or solid, Rev. Sci. Instrum. 67 (1) (1996) 29–35.
[14] D.G. Cahill, Thermal conductivity of thin films: measurements and understanding, J. Vacuum Sci. Technol. A 7 (3) (1989) 1259–1266.
[15] S.-M. Lee, D.G. Cahill, Heat transport in thin dielectric film, J. Appl. Phys. 81 (6) (1997) 2590–2595.
[16] J.H. Kim, A. Feldman, D. Novotny, Application of the three omega thermal conductivity measurement method to a film on a substrate of finite thickness, J. Appl. Phys. 86 (7) (1999) 3959–3963.
[17] T. Yamane, N. Nagai, S. Katayama, M. Todoki, Measurement of thermal conductivity of silicon dioxide thin films using a 3ω method, J. Appl. Phys. 91 (12) (2002) 9772–9776.
[18] C.E. Raudzis, F. Schatz, D. Wharam, Extending the 3ω method for thin-film analysis to high frequencies, J. Appl. Phys. 93 (10) (2003) 6050–6055.
[19] B.W. Olson, S. Graham, K. Chen, A practical extension of the 3ω method to multilayer structures, Rev. Sci. Instrum. 76 (5) (2005) 1–7. Article No. 053901.
[20] T. Tong, A. Majumdar, Reexamining the 3-omega technique for thin film thermal conductivity characterization, Rev. Sci. Instrum. 77 (10) (2006) 1–9. Article No. 104902.
[21] J. Alvarez-Quintana, J. Rodriguez-Viejo, Extension of the 3ω method to measure the thermal conductivity of thin films without a reference sample, Sensors Actuators A 142 (2008) 232–236.
[22] F. Chen, J. Shulman, Y. Xue, C.W. Chu, G.S. Nolas, Thermal conductivity measurement under hydrostatic pressure using the 3ω method, Rev. Sci. Instrum. 75 (11) (2004) 4578–4584.
[23] D.-W. Oh, A. Jain, J.K. Eaton, K.E. Goodson, J.S. Lee, Thermal conductivity of aluminum oxide nanofluids using the 3ω method, in: ASME International Mechanical Engineering Congress and Exposition, Chicago, Illinois, USA, November 2006, Paper No IMECE2006-14196.
[24] S.R. Choi, J. Kim, D. Kim, 3ω method to measure thermal properties of electrically conducting small-volume liquid, Rev. Sci. Instrum. 78 (8) (2007) 1–6. Article No. 084902.
[25] O. Bourgeois, T. Fournier, J. Chaussy, Measurement of the thermal conductance of silicon nanowires at low temperature, J. Appl. Phys. 101 (016104) (2007) 1–3.

[26] L. Lu, W. Yi, D.L. Zhang, 3ω method for specific heat and thermal conductivity measurements, Rev. Sci. Instrum. 72 (7) (2001) 2996–3003.
[27] T.Y. Choi, D. Poulikakos, J. Tharian, U. Sennhauser, Measurement of thermal conductivity of individual multiwalled carbon nanotubes by the 3-ω method, Appl. Phys. Lett. 87 (1) (2005) 1–3. Article No. 013108.
[28] X.J. Hu, A.A. Padilla, J. Xu, T.S. Fisher, K.E. Goodson, 3-omega measurements of vertically oriented carbon nanotubes on silicon, ASME J. Heat Transfer 128 (2006) 1109–1113.
[29] J. Hou, X. Wang, P. Vellelacheruvu, J. Guo, C. Liu, H.-M. Cheng, Thermal characterization of single-wall carbon nanotube bundles using the self-heating 3ω technique, J. Appl. Phys. 100 (12) (2006) 1–9. Article No. 124314.
[30] C. Dames, G. Chen, 1ω 2ω and 3ω methods for measurements of thermal properties, Rev. Sci. Instrum. 76 (124902) (2005) 1–14.
[31] K.D. Cole, Steady-periodic Green's functions and thermal-measurement applications in rectangular coordinates, ASME J. Heat Transfer 128 (2006) 709–716.
[32] J.-L. Battaglia, C. Wiemer, M. Fanciulli, An accurate low-frequency model for the 3ω method, J. Appl. Phys. 101 (10) (2007) 1–5. Article No. 104510.
[33] U.G. Jonsson, O. Andersson, Investigations of the low- and high-frequency response of 3ω-sensors used in dynamic heat capacity measurements, Meas. Sci. Technol. 9 (1998) 1873–1885.
[34] A. Jacquot, B. Lenoir, A. Dauscher, M. Stolzer, J. Meusel, Numerical simulation of the 3ω method for measuring the thermal conductivity, J. Appl. Phys. 91 (7) (2002) 4733–4738.
[35] T. Borca-Tasciuc, A.R. Kumar, G. Chen, Data reduction in 3ω method for thin-film thermal conductivity determination, Rev. Sci. Instrum. 72 (4) (2001) 2139–2147.
[36] P. Bhattacharya, S. Nara, P. Vijayan, T. Tang, W. Lai, P.E. Phelan, R.S. Prasher, D.W. Song, J. Wang, Characterization of the temperature oscillation technique to measure the thermal conductivity of fluids, Int. J. Heat Mass Transfer 49 (2006) 2950–2956.
[37] S.E. Gustafsson, E. Karawacki, Transient hot-strip probe for measuring thermal properties of insulating solids and liquids, Rev. Sci. Instrum. 54 (6) (1983) 744–747.
[38] M.N. Özisik, Heat Conduction, second ed., John Wiley and Sons, Inc., Berlin, 1993.
[39] MATLAB Function Reference. Available at: <http://www.mathworks.com/access/helpdesk/help/techdoc/matlab.html>, 2008.